GEOPHYSICS

Massive blow-out craters formed by hydrate-controlled methane expulsion from the Arctic seafloor

K. Andreassen,[1]* A. Hubbard,[1] M. Winsborrow,[1] H. Patton,[1] S. Vadakkepuliyambatta,[1] A. Plaza-Faverola,[1] E. Gudlaugsson,[1] P. Serov,[1] A. Deryabin,[2] R. Mattingsdal,[2] J. Mienert,[1] S. Bünz[1]

Widespread methane release from thawing Arctic gas hydrates is a major concern, yet the processes, sources, and fluxes involved remain unconstrained. We present geophysical data documenting a cluster of kilometer-wide craters and mounds from the Barents Sea floor associated with large-scale methane expulsion. Combined with ice sheet/gas hydrate modeling, our results indicate that during glaciation, natural gas migrated from underlying hydrocarbon reservoirs and was sequestered extensively as subglacial gas hydrates. Upon ice sheet retreat, methane from this hydrate reservoir concentrated in massive mounds before being abruptly released to form craters. We propose that these processes were likely widespread across past glaciated petroleum provinces and that they also provide an analog for the potential future destabilization of subglacial gas hydrate reservoirs beneath contemporary ice sheets.

Arctic continental shelves and land areas host vast amounts of methane trapped as hydrates, which are ice-like, solid mixtures of gas and water (*1*, *2*). Methane is a potent greenhouse gas, and sustained warming in the Arctic (*3*) has increased awareness that future destabilization of these shallow carbon reservoirs could cause a positive feedback to climate warming (*4*). Methane hydrate is stable within subseafloor sediments on continental margins worldwide, typically where water depths exceed 300 m and water temperatures are lower than ~5°C, whereas hydrates of heavier hydrocarbons are found at even shallower depths (*5*). Extensive gas hydrates also exist below permafrost on shallow Arctic continental shelves and land areas (*1*). Ice, permafrost, and gas hydrates combine to form a cryospheric cap that acts to trap natural gas leaking from underlying hydrocarbon reservoirs (*6*).

High levels of methane emissions from decomposing gas hydrates have been observed on the East Siberian Arctic Shelf (*7*) and on upper continental slopes worldwide (*2*), but there is no documented evidence that they affect the atmosphere (*2*). However, there is a large difference between slow, steady degassing (*8*) and the sudden, high-magnitude degassing events such as those that formed the large, 20- to 100-m-wide blow-out craters on the Russian Arctic Yamal and Gydan Peninsulas (*9*, *10*). Slow methane seepage from <200 m of water or on land does not appreciably contribute to the atmosphere because most of the methane is oxidized or dissolved into the sediments or water column (*2*), whereas abrupt blow outs would eject massive fluxes of methane into the ocean with a higher potential to attain the atmosphere. Such large methane-discharging craters, inferred to result from decomposing gas hydrates, have been reported both from Arctic marine (*11*, *12*) and land areas (*9*, *10*), but little is known about their formation.

We revisited a cluster of kilometer-wide craters in the northern Barents Sea (Fig. 1), inferred to have formed after deglaciation of the area ~15,000 years ago (*11*, *12*), in order to elucidate the processes and mechanisms of their formation. The investigation is based on new geophysical data from the subsurface, the seafloor, and water column, integrated with numerical modeling of the hydrate stability zone over the past 30,000 years, spanning full glacial to interglacial conditions (*13*). In the model, transient evolution of the hydrate system is determined by the diffusive heat transport through sediments and ice, subglacial and seafloor temperature variations, ice thickness, isostatic loading, and eustatic sea-level variations (*13*).

The study site is located within the Polar North Atlantic, in northern Bjørnøyrenna (Bear Island

[1]Centre for Arctic Gas Hydrate, Environment and Climate (CAGE), Department of Geosciences, UiT The Arctic University of Norway, N-9037 Tromsø, Norway. [2]Norwegian Petroleum Directorate, Harstad, Norway.
*Corresponding author. Email: karin.andreassen@uit.no

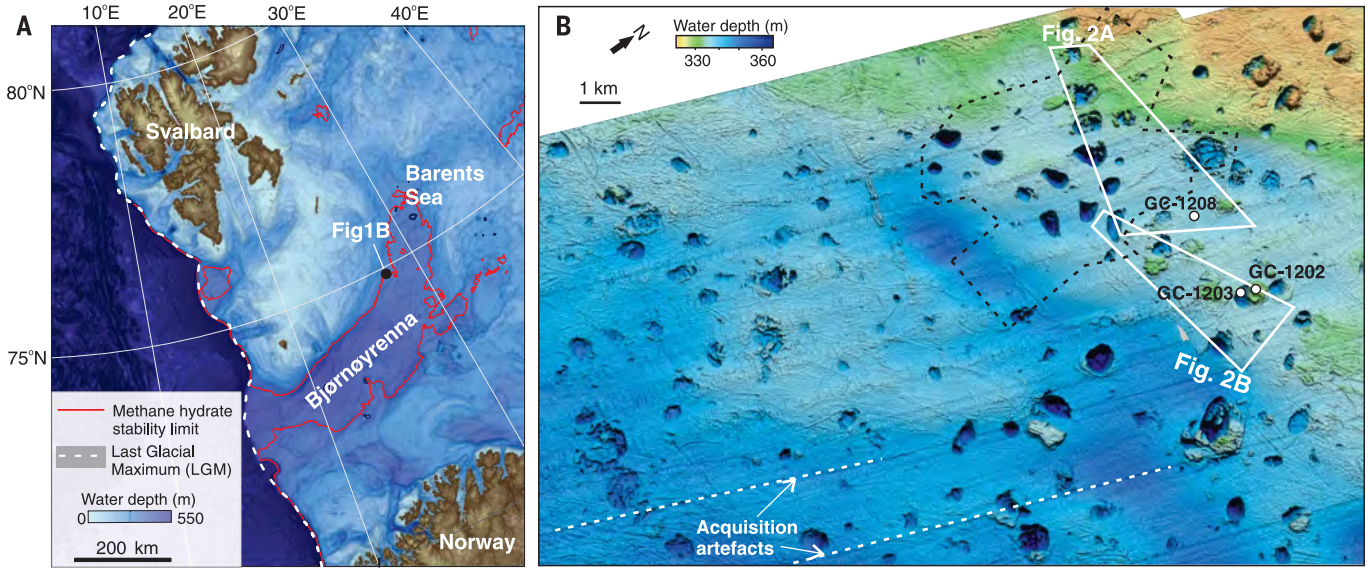

Fig. 1. Giant craters and mounds are located in the northern Barents Sea. (**A**) The Barents Sea Ice Sheet reached the continental shelf break during the LGM (*15*). Methane hydrate is currently stable in the deepest part of Bjørnøyrenna and other troughs of the Barents Sea (red polygons). (**B**) Giant craters and mounds within the local area of the study site. The black stippled polygon shows previous investigations of the area (*11*, *12*). White circles indicate locations of gas samples shown in tables S2 and S3.

Trough) on the contemporary methane hydrate stability boundary (Fig. 1A). The seafloor is generally smooth, sloping from 310 m below sea level in the north to 370 m below sea level in the south (Fig. 1B). The Barents Sea was extensively glaciated by a marine-based ice sheet that attained its peak during the Last Glacial Maximum (LGM) ~23,000 years before present (yr B.P.) (Fig. 1A). On retreat, the northwest sector of this ice sheet experienced a stepwise retreat through Bjørnøyrenna, with the study site deglaciating ~15,000 yr B.P. (*14*, *15*). The giant craters and mounds (Fig. 1B) are etched into sedimentary bedrock of Middle-Triassic age and are located on the western flank of a large anticline (fig. S1C). Extensive erosion throughout the Cenozoic has cut this stratigraphic structural high down to a series of well-developed clinoforms (fig. S1A). The topsets of these clinoforms have high potential for sands where fluids can migrate (*16*), whereas the bottomsets are an organically rich source of hydrocarbon fluids (*16*). A strategic petroleum industry borehole (7427/3-U-01) (fig. S1A) documents lithologies consisting predominantly of shale, coarsening upward into layers of fine sandstone (*17*). Seismic profiling indicates a series of faults and fractures leading upward from the Triassic hydrocarbon source and reservoir rocks directly into the seafloor craters and mounds (fig. S2C).

High-resolution bathymetry reveals more than 100 giant craters within a 440 km^2 area of the seafloor (Fig. 1B). The craters generally have an oval shape, between 300 and 1000 m in diameter and up to 30 m deep. Many have steep walls, with gradients up to 50°, but lack berms at their sides (Fig. 2, A and B; C3, C4, and C5). Others have a more complex morphology, typically with gently dipping sides, and often contain one or more internal mounds (Fig. 2A; C1 and C2). Analysis of chirp and seismic profiles verified against sediment cores reveals unlithified seafloor sediments to be <2 m thick. Numerous large seafloor mounds are also identified, mainly located at the flanks of the giant craters (Fig. 2B; M1 and M3). These mounds are up to 1100 m wide and 20 m high, generally semicircular to elliptical in plan form, and steep-sided and have an irregular upper surface incised with straight or curved furrows

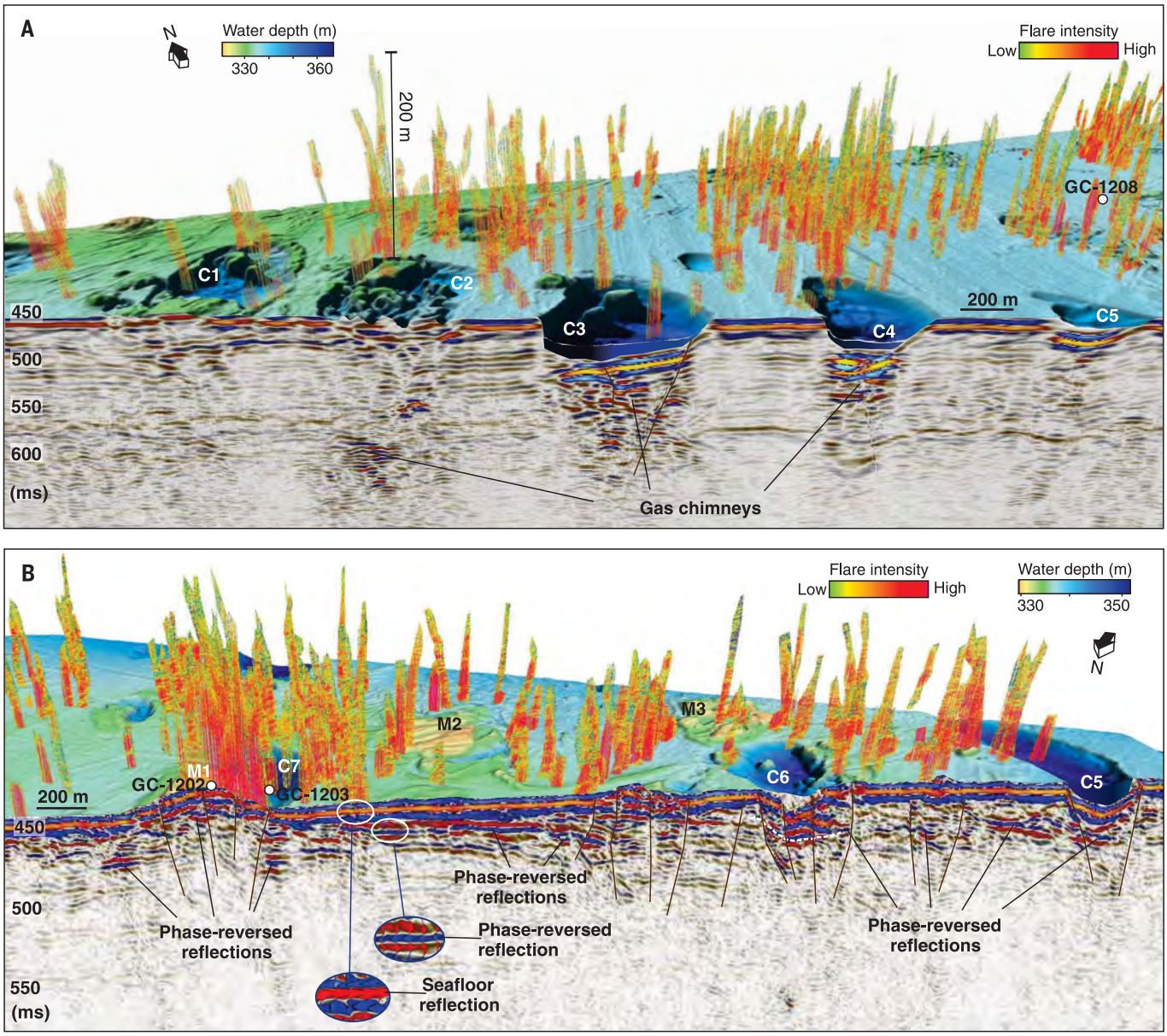

Fig. 2. Giant craters, mounds, and gas flares in the water and gas accumulations in the sediments. (**A** and **B**) Shaded relief bathymetry, combined with two-dimensional seismic profiles showing indications of gas in the sediments (phase-reversed reflection and gas chimneys). Faults are indicated by brown lines. White circles indicate locations of gas samples shown in tables S2 and S3.

(fig. S2D; M1 to M6). Some of the furrows are iceberg scours, whereas others are associated with subcropping fractures and erosion pits formed by gas escape along faults and fractures. Smaller craters and mounds between 50 and 200 m wide with varying relief are abundant across the study site, clustered around and within the larger craters (Fig. 2 and fig. S2, B and D).

More than 600 gas flares are identified as water column acoustic anomalies in echo-sounder profiles (Fig. 2, A and B, red to yellow columns) because of strong velocity/density contrasts between chains of gas bubbles and the water-column. Single flares are typically 50 to 200 m wide and rise to ~200 m into the water column (Fig. 2A). The majority of flares emerge around and between craters and mounds, whereas some originate from within the craters and mounds themselves (Fig. 2). We interpret the presence of strong seismic reflections with a phase-reversed polarity compared with seafloor reflections as free gas accumulations in the subseafloor sediments (Fig. 2B) (*18*). Such free gas accumulations are also observed in vertical zones (gas chimneys) with high-amplitude, chaotic seismic reflection patterns below the craters (Fig. 2A). These chimneys appear where natural gas distributes into irregular patches in fractured, low-permeable shales (*18*).

Measurements acquired directly from seafloor sediments (Fig. 2) indicate that 97% of the gas present at mound M1 is methane, with 2.5% ethane and propane (table S2, GC 1202). Because of its heavier hydrocarbon content, this natural gas is stable as structure II hydrates (*5*) under present seafloor depth and temperature conditions (Fig. 3A, purple line year 0). However, gas sampled from crater C7 (Fig. 2B, GC1203) is almost pure methane, with just 0.1% heavier hydrocarbon (table S2, GC1203) and hence is unstable in hydrate form under present seafloor conditions (Fig. 3A, black stippled line). Analysis of gas ratios (table S2) indicates a thermogenic origin for the natural gas and associated hydrates, in which organic molecules are broken down under high-temperature, high-pressure conditions at subsurface depths typically exceeding 1 km (*19*).

Because the observed mounds are elevated well above the surrounding seafloor, any plausible formation mechanism must either deposit material on the existing seafloor or otherwise uplift the existing sedimentary bedrock. The absence of any discernible seismic paleo-seafloor reflections from the base of the mounds (Fig. 2B, M1) and a distinct lack of extrusive features such as mud flows and mud cones discount extrusive processes (*20*). Ejecta deposits sourced from the adjacent craters (*11*) would likewise have a clear basal reflection, as would carbonate and/or coral mounds (*21*). The lack of a basal reflector, combined with the presence of actively venting natural gas connected to deeper hydrocarbon sources, leads us to assert that the giant mounds we observed were formed by the growth of gas hydrate accumulations within the subsurface. Similar but smaller mounds have been observed elsewhere and are often referred to as gas hydrate pingos (*20*).

We propose a conceptual model that links the formation of these hydrate pingos with the giant craters through the build-up and subsequent dissociation of gas hydrates (Fig. 3). Cyclic episodes of Barents Sea ice sheet loading and unloading throughout the Pleistocene caused repeated pressurization and depressurization of the underlying thermogenic hydrocarbon reservoirs. This would have driven large fluxes of natural gas upward into the near subsurface (*22*), with gas migration focused into the crater and mound area by the

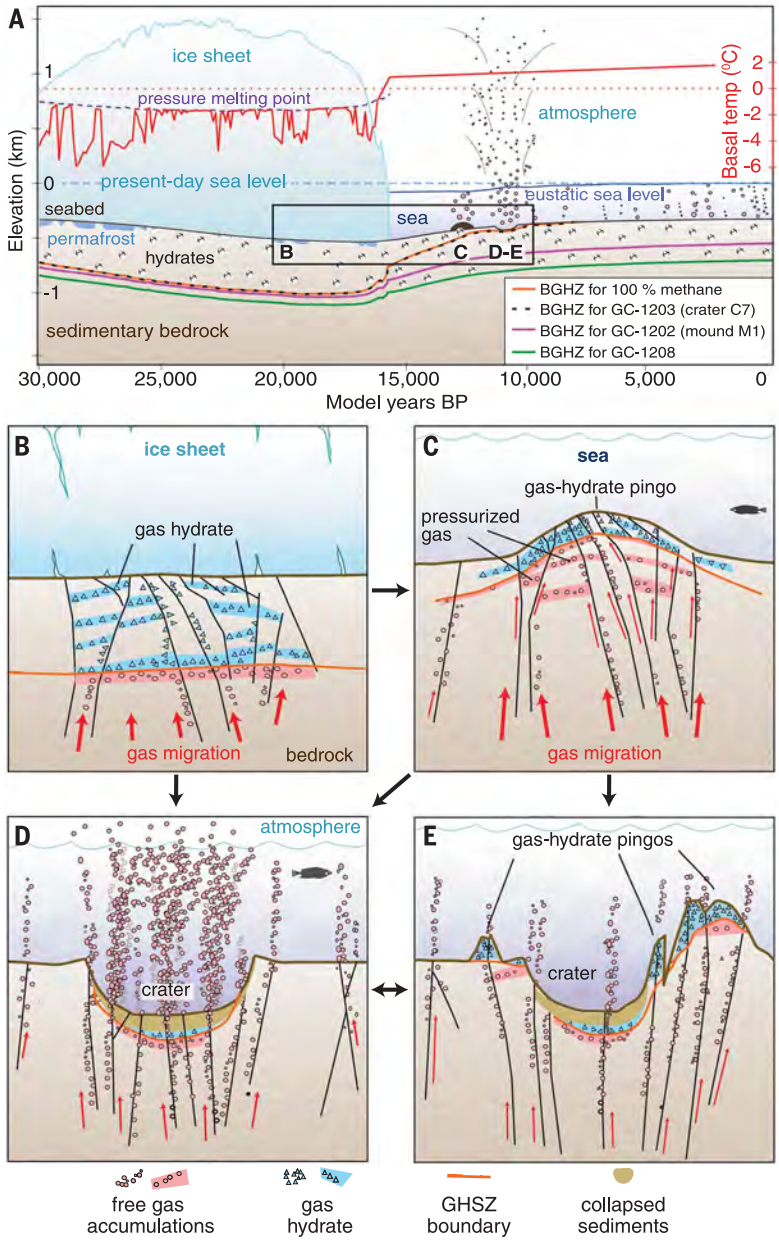

Fig. 3. Conceptual sketch for formation of craters and mounds in the northern Barents Sea. (**A**) Numerical model of thickness for the ice sheet (*15*), the gas hydrate stability zone for different gas compositions and subglacial permafrost over the past 30,000 years. The model values are calculated at the location of mound M1 (Fig. 2B). The base of the gas hydrate stability zones (BGHZs) are calculated for gas compositions measured in the seafloor sediments (table S2) and for pure methane. (**B**) Ice loading, focused gas migration along faults and fractures from deeper hydrocarbon reservoirs, and formation of subglacial gas hydrate and free gas accumulations. (**C**) The ice sheet retreats and sediment pore pressure is drastically reduced. This leads to decomposition of gas hydrates at depth, build up of overpressurized gas below a shallowing gas hydrate zone with increased gas hydrate concentration, and formation of a gas hydrate pingo. (**D**) Collapse of gas hydrate pingo because of hydrate dissociation, leading to crater formation. (**E**) Collapsed sediments and gas hydrates in the crater partially block upward gas flow, which is diverted to the crater flanks. GHSZ, gas hydrate stability zone.

morphology of the deeper Middle Triassic anticline structure (fig. S1, A and C). Subglacial conditions associated with a ~2-km-thick ice sheet during the LGM (*13*) acted to stabilize methane hydrate formation within the upper ~440 m of subseafloor sediments (Fig. 3A, orange line). Heavier hydrates were stable down to ~520 m (Fig. 3A, green line). Lateral sequestration of gas hydrates within the coarse-grained porous bedrock were accompanied by the build-up of free natural gas accumulations in faults and fractures below the hydrate stability zone (Fig. 3B).

The rapid transition of the seafloor from a subglacial to marine environment when the ice sheet retreated abruptly degraded conditions conducive for hydrate stability, forced by a dramatic reduction in loading, hydrostatic pressure and increase in temperature (Fig. 3A). Between 17,000 and 15,000 years ago, the methane-hydrate stability zone diminished from ~440 to ~200 m (Fig. 3A, orange line), causing deeper hydrates to decompose, migrate upward, and recrystallize at shallower depths (*13*). This resulted in an increased volume of gas concentrated within a progressively thinning and shallowing gas hydrate stability zone. This volume expansion due to gas hydrate regrowth, along with a buildup of underlying pressurized free gas, led to the development of the gas hydrate pingos (Fig. 3C) (*20*). Driven by ongoing isostatic rebound and inflow of warm North Atlantic water, the methane hydrate stability zone continued to thin to ~30 m by 12,000 yr B.P. (Fig. 3A, orange and black stippled lines), despite eustatic sea level rise. Last, the release of gas from decomposed hydrate accumulations drove hydrofractures through the overburden rocks and sediment, triggering multiple methane-release events and creating abrupt gas expulsions. These expulsion events eroded and deformed the fractured sediments, promoting overlying seafloor blow out, collapse of hydrate pingos, and formation of the massive craters observed today (Fig. 3D) (*23*).

The appearance of gas chimneys under most of the craters and gas flares around and on the flanks of craters (Fig. 2) implies that upward gas migration pathways through the craters became partially blocked. The plugging of gas flow pipes after blow out and formation of new pipes adjacent to old ones to release rising gas pressure have been suggested in other blow-out settings (*23*). When combined, these processes explain the development of the system of giant craters with underlying, interconnected pipes and the distribution of smaller mounds and craters on the flanks of the larger craters (Fig. 3E) that act to promote further crater expansion (Fig. 2).

The craters and mounds cut across, and therefore post-date megascale glacial lineations (MSGLs)—landforms developed beneath the fast-flowing Bjørnøyrenna ice stream (fig. S2D, black lines) (*14*). Iceberg ploughmarks can also be observed to erode and incise the tops of mounds, with some tracking down into and across craters (fig. S2D, stippled white lines) signifying that the craters and mounds formed while icebergs with keels between 300 and 400 m deep were active in the Barents Sea. We can hence constrain the timing of crater and mound formation to a relatively short time window after the onset of local ice-free conditions around 15000 yr B.P., but before or during the final stages of ice stream retreat from northern Bjørnøyrenna ~11,600 years ago (*24*). This chronology is entirely consistent with our modeling of the rapid thinning of the methane hydrate stability zone from 15,000 to 12,000 years, with the final stages of decomposition by 11,000 years ago (Fig. 3A, orange and stipple-black lines).

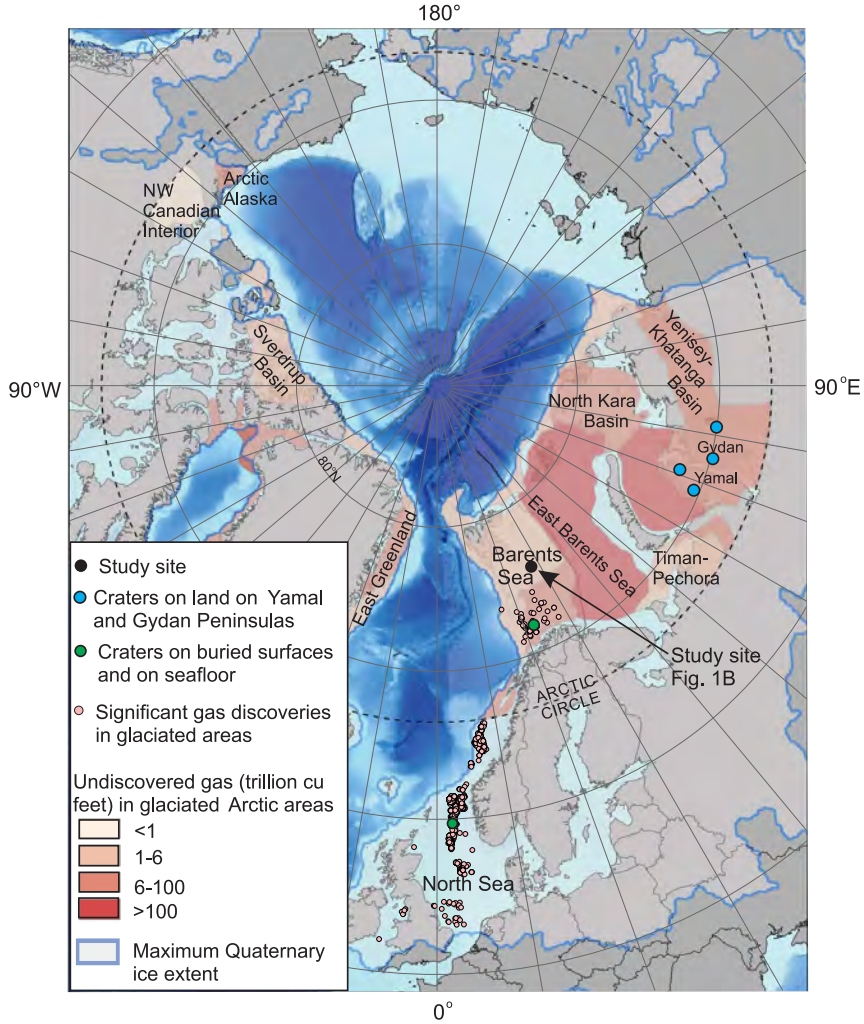

Fig. 4. Arctic petroleum basins that have been covered by grounded ice during the Quaternary. Areas north of the Arctic Circle with high estimates of undiscovered gas (*36*) that have been covered by a grounded ice sheet during the Quaternary (*35*) are indicated in pink to dark red colors. Gas discoveries in the Barents Sea and North Sea are from the Norwegian Petroleum Directorate (www.npd.no) and the British government (www.gov.uk/oil-and-gas). Giant craters on the seafloor and buried glaciated surfaces in the Barents Sea (*30*) and North Sea (*31*), as well as craters on land on the Russian Yamal and Gydan Peninsulas (*9*), are indicated.

The primary drivers for gas hydrate dissociation and gas expulsion varied in space and time over the glaciated Barents Sea but were critically controlled, either directly or indirectly, by ice sheet evolution. At the study area, depressurization owing to the loss of subglacial loading of ~1950-m-thick ice, greatly exceeded any hydrostatic compensation associated with changes in relative sea level (+115 m eustatic sea level rise and –205 m in isostatic depression) since the LGM. On deglaciation of our study area, the impact of isostatic loading left the water depth at ~440 m, still some ~115 m greater than today despite the eustatic sea level being 80 m lower at the time. The temperate (at pressure-melting point) subglacial conditions associated with the Bjørnøyrenna ice stream precluded the development of a thick permafrost horizon even during LGM conditions (Fig. 3A, permafrost). Rapid retreat of the actively calving Bjørnøyrenna ice stream was partially driven by the ingress of relatively warm Atlantic water (*25*), which also adversely influenced the stability of sequestered seafloor hydrates (Fig. 3A, red basal temperature curve).

The presence of active contemporary gas flares demonstrates continued slow methane release across the study area. Geological analogs of slow and sustained, fluid-flow events southwest of the area have recently been dated by using authigenic

carbonate crusts. Here, methane release commenced after the ice sheet retreated and continued for up to 10,000 years (*26*) at flow rates of 20 to 60 cm per year (*27*). Our analysis suggests that glaciated petroleum provinces are preconditioned to sequester large fluxes of methane subglacially, in extensive, but heterogeneously distributed, gas hydrate accumulations. Upon ice sheet retreat, these gas hydrates dissociate, forming surface expressions such as gas hydrate pingos, which eventually collapse into craters, releasing large fluxes of methane. Gas hydrate pingos are some of the most climatically sensitive settings because they often contain shallow and relatively pure methane hydrate (*28*) that can dissociate rapidly in response to even moderate environmental perturbations (*29*).

The gas stored within the Bjørnøyrenna pingos built up until it over-pressurized and subsequently abruptly vented, releasing massive volumes of methane. Major methane-venting events analogous to this appear to be rare but may easily be overlooked because of high rates of postglacial deposition limiting their exposure in the geological record. Previous identification of craters of similar size and morphology as those identified in this study, but found on buried glacial surfaces farther south in the Barents and North Seas (Fig. 4, green dots) (*30*, *31*), supports this proposition. Despite their apparent infrequency, the net impact of such high-magnitude blow-out events may still be greater than the sustained but gradual seepage, for which there is abundant evidence in the geological record (*2*, *8*, *26*).

Seafloor craters and/or hydrate mounds are commonly associated with gas seepage at petroleum provinces elsewhere, such as the Gulf of Mexico (*28*, *32*, *33*) and the West African continental margin of Congo (*34*), Nigeria (*23*), and Angola (*20*). Many of these features are similar to those at our study site and likewise are related to seafloor doming and blow out by overpressured natural gas. However, these craters and mounds appear in tropical oceanic settings where the seafloor is several thousand meters deep and well within the stability field of gas hydrates, so their formation must be caused by processes other than deglaciation and hydrate destabilization. Here, we propose a conceptual model that links large-scale seafloor methane expulsion to processes related to ice sheet retreat, resulting in destabilization of shallow, high-latitude gas hydrate systems.

Thermogenic gas reservoirs have been confirmed, and more are evident beneath glaciated continental margins across the Arctic and elsewhere (Fig. 4, pink to dark red areas). We estimate that a 33 million km^2 area (*35*) of confirmed hydrocarbon reserves off the United States, Canada, Russia, and northwest Europe (*13*, *36*) was directly influenced by grounded ice sheets during the past glaciation. This vast tract experienced ideal high-pressure/low-temperature subglacial conditions conducive to sequestration of methane and heavier natural gases in hydrate form. Analogous to our study here, such hydrates would likewise have been subject to similar deglaciation-triggered decomposition, followed by large-scale gas expulsion. Given the relatively shallow and abrupt nature of this expulsion, it remains to be seen whether such methane release could have attained or affected the atmosphere. Either way, the seafloor craters documented here and identified at similarly glaciated margins underlain by thermogenic hydrocarbon reservoirs elsewhere (Fig. 4) reveal that ice sheets promote subglacial natural gas sequestration in hydrate form and its subsequent large-scale release upon deglaciation. Hence, the conceptual model presented here (Fig. 3) also delivers a benchmark for the destabilization of gas-hydrate reservoirs inferred to exist beneath today's Antarctic and Greenland ice sheets (*6*, *37*) that are currently experiencing ongoing and projected future retreat (*3*).

REFERENCES AND NOTES

1. K. A. Kvenvolden, *Chem. Geol.* **71**, 41–51 (1988).
2. C. D. Ruppel, J. D. Kessler, *Rev. Geophys.* **55**, 126–168 (2017).
3. Intergovernmental Panel on Climate Change (IPCC), Climate Change 2013: The Physical Science Basis. Contribution of Working Group I, in *Fifth Assessment Report of the Intergovernmental Panel on Climate Change*, T. F. Stocker *et al.*, Eds. (Cambridge Univ. Press, 2013).
4. E. G. Nisbet, J. Chappellaz, *Science* **324**, 477–478 (2009).
5. E. D. Sloan, C. A. Koh, *Clathrate Hydrates of Natural Gases* (CRC Press, ed. 3, 2008).
6. K. M. Walter Anthony, P. Anthony, G. Grosse, J. Chanton, *Nat. Geosci.* **5**, 419–426 (2012).
7. N. Shakhova *et al.*, *Science* **327**, 1246–1250 (2010).
8. G. K. Westbrook, K. E. Tatcher, E. J. Rohling, *Geophys. Res. Lett.* **36**, L15608 (2009).
9. V. Bogyavleski, *GEO ExPro*, **12**, 75–78 (2015); www.geoexpro.com/articles/2015/12/gas-blowouts-on-the-yamal-and-gydan-peninsulas.
10. M. O. Leibman, A. I. Kizyakov, A. V. Plekhanov, I. D. Streleskaya, *Geogr. Environ. Sustain.* **7**, 68–80 (2014); www.geogr.msu.ru/GESJournal/contents.php?iid=22&menupos=7.
11. A. Solheim, A. Elverhøi, *Geo-Mar. Lett.* **13**, 235–243 (1993).
12. S. Lammers, E. Suess, M. Hovland, *Geol. Rundsch.* **84**, 59–66 (1995).
13. Materials and methods are available as supplementary materials.
14. M. C. M. Winsborrow, K. Andreassen, G. Corner, J. S. Laberg, *Quat. Sci. Rev.* **29**, 424–442 (2010).
15. H. Patton, A. Hubbard, K. Andreassen, M. Winsborrow, A. P. Stroeven, *Quat. Sci. Rev.* **153**, 97–121 (2016).
16. T. Høy, B. A. Lundschien, *Geol. Soc. London Mem.* **35**, 249-260 (2011).
17. B. A. Lundschien, T. Høy, A. Mørk, *Norw. Pet. Dir. Bull.* **11**, 3–20 (2014).
18. H. Løseth, M. Gading, L. Wensaas, *Mar. Pet. Geol.* **26**, 1304–1319 (2009).
19. K. A. Kvenvolden, T. M. Vogel, J. V. Gardner, *J. Geochem. Explor.* **14**, 209–219 (1981).
20. C. Serié, M. Huuse, N. S. Schødt, *Geology* **40**, 207–210 (2012).
21. E. Le Guilloux *et al.*, *Deep Sea Res. Part II Top. Stud. Oceanogr.* **56**, 2394–2403 (2009).
22. I. Yu, Z. Lerche, B. Torudbakken, R. O. Thomsen, *Mar. Pet. Geol.* **14**, 277–338 (1997).
23. H. Løseth *et al.*, *Mar. Pet. Geol.* **28**, 1047–1060 (2011).
24. K. Andreassen, M. C. M. Winsborrow, L. R. Bjarnadóttir, D. C. Rüther, *Quat. Sci. Rev.* **92**, 246–257 (2014).
25. D. K. Kristensen, T. L. Rasmussen, N. Koç, *Boreas* **42**, 798–813 (2013).
26. A. Crémière *et al.*, *Nat. Commun.* **7**, 11509 (2016).
27. R. Luff, K. Wallmann, G. Aloisi, *Earth Planet. Sci. Lett.* **221**, 337–353 (2004).
28. I. R. MacDonald *et al.*, *Geology* **22**, 699–702 (1994).
29. C. D. Ruppell, *Nature Edu. Knowl.* **3**, 29 (2011).
30. I. Ostanin, Z. Anka, R. di Primio, A. Bernal, *Mar. Pet. Geol.* **43**, 127–146 (2013).
31. C. Fichler, S. Henriksen, H. Rueslaatten, M. Hovland, *Petrol. Geosci.* **11**, 331–337 (2005).
32. D. B. Prior, E. H. Doyle, M. J. Kaluza, *Gulf Mex. Sci.* **243**, 517–519 (1989).
33. F. J. Rocha-Legorreta, *Leading Edge (Tulsa Okla.)* **28**, 714–717 (2009).
34. A. Gay, M. Lopez, C. Berndt, M. Séranne, *Mar. Geol.* **244**, 68–92 (2007).
35. J. Ehlers, P. L. Gibbard, *Quat. Int.* **164-165**, 6–20 (2007).
36. D. L. Gautier *et al.*, *Science* **324**, 1175–1179 (2009).
37. J. L. Wadham *et al.*, *Nature* **488**, 633–637 (2012).

ACKNOWLEDGMENTS

This work was supported by the Research Council of Norway (RCN) through its Centres of Excellence funding scheme, project no. 223259. Norwegian Petroleum Directorate kindly provided the petroleum industry multichannel seismic data. We thank the officers and crew of *R/V Helmer Hanssen* and engineer S. Iversen for helping with the collecting and processing of data. Supplementary data are available at http://opendata.uit.no.

SUPPLEMENTARY MATERIALS

www.sciencemag.org/content/356/6341/948/suppl/DC1
Materials and Methods
Supplementary Text
Figs. S1 to S3
Tables S1 to S4
References (*38*–*63*)

23 November 2016; accepted 11 May 2017
10.1126/science.aal4500

Massive blow-out craters formed by hydrate-controlled methane expulsion from the Arctic seafloor

K. Andreassen, A. Hubbard, M. Winsborrow, H. Patton, S. Vadakkepuliyambatta, A. Plaza-Faverola, E. Gudlaugsson, P. Serov, A. Deryabin, R. Mattingsdal, J. Mienert and S. Bünz (June 1, 2017) *Science* **356** (6341), 948-953. [doi: 10.1126/science.aal4500]

Editor's Summary

Methane takes the quick way out

Accounting for all the sources and sinks of methane is important for determining its concentration in the atmosphere. Andreassen *et al.* found evidence of large craters embedded within methane-leaking subglacial sediments in the Barents Sea, Norway. They propose that the thinning of the ice sheet at the end of recent glacial cycles decreased the pressure on pockets of hydrates buried in the seafloor, resulting in explosive blow-outs. This created the giant craters and released large quantities of methane into the water above.

Science, this issue p. 948

This copy is for your personal, non-commercial use only.

Science (print ISSN 0036-8075; online ISSN 1095-9203) is published weekly, except the last week in December, by the American Association for the Advancement of Science, 1200 New York Avenue NW, Washington, DC 20005. Copyright 2016 by the American Association for the Advancement of Science; all rights reserved. The title *Science* is a registered trademark of AAAS.